

## **General Disclaimer**

### **One or more of the Following Statements may affect this Document**

- This document has been reproduced from the best copy furnished by the organizational source. It is being released in the interest of making available as much information as possible.
- This document may contain data, which exceeds the sheet parameters. It was furnished in this condition by the organizational source and is the best copy available.
- This document may contain tone-on-tone or color graphs, charts and/or pictures, which have been reproduced in black and white.
- This document is paginated as submitted by the original source.
- Portions of this document are not fully legible due to the historical nature of some of the material. However, it is the best reproduction available from the original submission.

## SPACE EXPLORATION: A RISK FOR NEURAL STEM CELLS

JUAN M. ENCINAS<sup>1</sup>, MARCELO E. VAZQUEZ<sup>2</sup>, ROBERT C. SWITZER<sup>3</sup>, DENNIS W.  
CHAMBERLAND<sup>4</sup>, HARRY NICK<sup>5</sup>, HOWARD G. LEVINE<sup>4</sup>, PHILIP J. SCARPA<sup>4</sup>, GRIGORI  
ENIKOLOPOV<sup>1</sup>, AND DENNIS A. STEINDLER<sup>5</sup>

<sup>1</sup>COLD SPRING HARBOR LABORATORY, <sup>2</sup>BROOKHAVEN NATIONAL LABORATORY,  
<sup>3</sup>NEUROSCIENCE ASSOCIATES INC., <sup>4</sup>NASA KENNEDY SPACE CENTER, <sup>5</sup>MCKNIGHT BRAIN  
INSTITUTE

During spaceflights beyond low Earth orbit, astronauts are exposed to potentially carcinogenic and tissue damaging galactic cosmic rays, solar proton events, and secondary radiation that includes neutrons and recoil nuclei produced by nuclear reactions in spacecraft walls or in tissue (1). Such radiation risk may present a significant health risk for human exploration of the moon and Mars. Emerging evidence that generation of new neurons in the adult brain may be essential for learning, memory, and mood (2) and that radiation is deleterious to neurogenesis (3-5) underscores a previously unappreciated possible risk to the cognitive functions and emotional stability of astronauts exposed to radiation in space. Here we use a novel reporter mouse line to identify at-risk populations of stem and progenitor cells in the brain and find, unexpectedly, that quiescent stem-like cells (rather than their rapidly dividing progeny) in

the hippocampus constitute the most vulnerable cell population. This finding raises concerns about the possible risks facing astronauts on long duration space missions.

To simulate the space radiation environment, we exposed nestin-CFPnuc mice (6) to 100 cGy doses of 1 GeVn  $^{56}\text{Fe}$  ions (doses corresponding to an average fluence of 1-3 hits per cell). Brains were analyzed using immunocytochemistry and stereology (see supporting online material). Exposure to radiation resulted in a dramatic decrease (65%,  $p=0.00012$ ) in the number of BrdU-positive cells in the dentate gyrus (DG) ( $1704\pm231$  vs.  $600\pm95$ ); in all cases, BrdU-positive cells were positioned in the subgranular zone (SGZ) and only occasionally in the hilus (Fig. 1a,b,e,h). Radiation also decreased the number of nestin-CFPnuc-expressing neural precursor cells in the DG by 38% ( $15076\pm2338$  vs.  $9436\pm1847$ ;  $p=0.0081$ ; Fig. 1b,f,g,i,j). Expression of CFP marks two classes of precursors in the DG of nestin-CFPnuc animals, the quiescent neuronal progenitors (QNPs) and the amplifying neuronal progenitors (ANPs) (6). Of these, the reduction in the number of QNPs after irradiation was the most pronounced (45% decrease,  $9386\pm1905$  vs.  $5180\pm1462$  cells;  $p=0.0128$ ; Fig. 1c), whereas the number of ANPs decreased by 25% ( $5690\pm766$  vs.  $4256\pm660$ ;  $p=0.0297$ ; Fig. 1d).

The changes in the populations of early progenitors were also reflected in the number of dying cells in the brain, as revealed by amino cupric silver and caspase-3 staining (Fig. 1k-m). The increase in cell degeneration was observed selectively in the neurogenic areas, especially in the SGZ, where QNP and ANP cells are located, thus confirming the observed reduction in nestin-CFPnuc cells. Furthermore, we observed activated Iba1-

positive microglial cells and cells resembling infiltrating macrophages selectively located in the SGZ (Fig. 1n-p). These degeneration- and inflammation-related changes were observed 6 h after irradiation but not 24 h or 3 weeks after irradiation.

Our results show that QNPs, a population of stem-like cell in the hippocampus, is selectively affected by the type of radiation that manned missions may expect during space exploration. The concomitant loss of ANPs was expected since they represent a rapidly dividing cell population that is thus susceptible to various types of radiation. However, the finding that QNP cells, despite their low division rate, are particularly vulnerable to space radiation, was unexpected. This suggests that additional mechanisms, not directly related to cell replication, may be responsible for this selective loss. Importantly, if the loss of this most primitive and normally non-self-renewable progenitor class in the hippocampus is not compensated (e.g., by increasing the rate of asymmetric divisions of the remaining QNPs or restoring their number through symmetric divisions), the number of new neurons and later, of all granule neurons in the DG may decline. Given the increasing evidence pointing to the role of adult neurogenesis in memory and mood control, the risk to these cells represents an important factor to consider when planning manned space missions. Further investigations should address the issue of whether a reduced flux expressed over a longer period would have the same effects as the acute exposure used in these experiments. Our model offers a ground-based radiation-exposure test system that will help to assess radiation risk and to develop countermeasures, such as shielding and radioprotective drugs.

## **ACKNOWLEDGMENTS**

We thank Barbara Mish, Adele Billups, Laura Thompson and Beatrice Pyatt for their assistance with the experiments and Julian Banerji for discussions and comments. J.M.E. is a fellow of the Ministerio de Educación y Ciencia of Spain. Support to G.E. was provided by the Ira Hazan Fund and The Seraph Foundation and to D.S by NINDS grant NS37556 and NHLBI grant 70143. This study was supported by grants from the Florida Space Research Institute, NASA Radiation Health Program and the National Space Biomedical Research Institute.

## FIGURE LEGENDS

### Figure 1.

**a-d.**  $^{56}\text{Fe}$  radiation decreases the number of BrdU-labeled cells (a), nestin-CFPnuc cells (b), QNP cells (c), and ANP cells (d) in the DG of nestin-CFPnuc mice. Mice were irradiated, injected with BrdU, and sacrificed 24 hours later. White bars correspond to the control group (C) and grey bars to the irradiated group (R). The results for individual animals are shown as black dots. Error bars show s.e.m. \* $p \leq 0.05$ , \*\* $p \leq 0.01$ , \*\*\* $p \leq 0.0005$ .

**e-j.** Representative photomicrographs of DG sections from control (e, f, g) and irradiated (h, i, j) animals. (e and h) – sections stained for BrdU; dashed line outlines the external limits of the DG. (f, g, i, j) – QNP and ANP cells at lower (f, g) and higher (i, j) magnification. The soma and the nuclei (visualized by immunostaining against CFP) of both QNPs and ANPs are located in the subgranular zone. QNPs extend apical processes (immunostained with antibody to vimentin) which cross the granule cell layer and can thus be differentiated from the ANPs (arrows).

**k-m.** Amino-cupric-silver stain for cell degeneration (k, l) and anti-caspase-3 staining for apoptotic cells (m) in the DG of control (k) and irradiated (l, m) mice, showing cell degeneration and apoptosis after irradiation.

**n-p.** Staining for microglial cells with anti-Iba1 antibody in the DG of control (n) and irradiated (o,p) mice; note altered morphology of microglial cells after irradiation.

Scale bars are 20  $\mu\text{m}$  in *e, f, h, i, k-o*, 5  $\mu\text{m}$  in *g* and *j*, and 10  $\mu\text{m}$  in *p*.

## REFERENCES

1. F. A. Cucinotta, M. Durante, *Lancet Oncol* **7**, 431 (May, 2006).
2. G. L. Ming, H. Song, *Annu Rev Neurosci* **28**, 223 (2005).
3. G. P. Marshall, 2nd, E. W. Scott, T. Zheng, E. D. Laywell, D. A. Steindler, *Stem Cells* **23**, 1276 (Oct, 2005).
4. S. Mizumatsu *et al.*, *Cancer Res* **63**, 4021 (Jul 15, 2003).
5. M. L. Monje, S. Mizumatsu, J. R. Fike, T. D. Palmer, *Nat Med* **8**, 955 (Sep, 2002).
6. J. M. Encinas, A. Vaahtokari, G. Enikolopov, *Proc Natl Acad Sci U S A* **103**, 8233 (May 23, 2006).

## Supplemental Material: MATERIALS AND METHODS

**Transgenic mice.** For evaluating the effect of radiation on neural stem and progenitor cells we used a nestin-CFPnuc reporter mouse line (1). These transgene mice were generated by a pronuclear injection into the fertilized oocytes from C57BL/6xBalb/cBy hybrid mice of a construct encoding CFP with nuclear localization domain, whose expression was regulated by the promoter and the second intron of the nestin gene and polyadenylation sequences from simian virus 40. Transgenic mice were repeatedly mated with C57BL/6 mice for more than 7 generations. The use of this reporter line for examining changes in adult neurogenesis is described in detail elsewhere (1). Use of animals was reviewed and approved by the Cold Spring Harbor Laboratory, Brookhaven National Laboratory and Kennedy Space Center Animal Use and Care Committees.

**Irradiation and analysis.** Two-month old nestin-CFPnuc mice were irradiated head alone under anesthesia (isofluorane) at the NASA Space Radiation Laboratory, Upton New York. Mice were exposed to 0, 50 and 100 cGy of 1 GeV/n Fe ions (LET: 148 keVp/ $\mu$ m), injected with BrdU (150 mg/kg), and sacrificed 24 h later. Mice were administered an overdose of chloral hydrate, and the tissues were fixed by transcardial perfusion with 30 ml of PBS, pH 7.4 followed by 30 ml of 4% (w/v) paraformaldehyde in PBS. The brains were removed, cut longitudinally into two hemispheres and postfixed with the same fixative for 3 h at room temperature, then transferred to PBS, and kept at 4°C. Serial sagittal sections, 50- $\mu$ m thick, were obtained using a Vibratome 1500 (Vibratome, St. Louis, MO). For the amino-cupric-silver and caspase-3 staining of cell degeneration, brains were treated overnight with 20% glycerol and 2% dimethylsulfoxide



to prevent freeze-artifacts and embedded in a gelatin matrix using MultiBrain™ Technology (NeuroScience Associates, Knoxville, TN). After curing, the block was rapidly frozen by immersion in isopentane chilled to -70°C with crushed dry ice, mounted on a freezing stage of an AO 860 sliding microtome and sectioned. Sections were collected sequentially into a 4x5 array of containers filled with Antigen Preserve solution (50% PBS pH 7.0, 50% Ethylene glycol, 1% Polyvinyl Pyrrolidone) for immunohistochemistry. The containers to be used for amino-cupric-silver staining (2) were filled with 4% formaldehyde in 1.4% sodium cacodylate buffer, pH 7.4. After mounting, the sections were air dried, counterstained with neutral red, dehydrated, cleared in xylene and coverslipped.

Immunostaining was carried out following a standard procedure. The sections were incubated with blocking and permeabilization solution (PBS containing 0.2 % Triton-100X and 3% BSA) for 1 h at room temperature and then incubated overnight at 4°C with the primary antibodies (diluted in the same solution). After thorough washing with PBS, sections were incubated with secondary antibodies in PBS for 1 h at room temperature in darkness. After washing with PBS, the sections were mounted on gelatine-coated slides with DakoCytomation Fluorescent Mounting Medium (DakoCytomation, Carpinteria, CA). Those sections that were designated for the analysis of BrdU incorporation, were treated, before the immunostaining procedure, with 2M HCl for 30 min at 55°C, rinsed with PBS, treated with 1mM sodium tetraborate for 10 min at room temperature, and washed with PBS. For diaminobenzidine staining, the secondary antibodies were incubated in PBS for 1 h at room temperature. After washing, the sections were

incubated with peroxidase-linked ABC (Vector Laboratories, Burlingame, CA.). The peroxidase activity was revealed using the Sigma Fast 3,3'-diaminobenzidine tetrahydrochloride with metal enhancer tablet set (Sigma-Aldrich, St Louis, MO). Following antibodies were used: chicken anti-GFP (Aves Laboratories, Tigard, OR) diluted 1:500; chicken anti-vimentin (Chemicon International, Temecula, CA) diluted 1:500; rat anti-BrdU (Serotec, Raleigh, NC) diluted 1:400; rabbit anti-caspase-3 (Cell Signaling, Beverly, MA) diluted 1:1000, rabbit anti-Iba1 (Wako, Richmond, VA) diluted 1:5000, AlexaFluor 488 goat anti-rat (Molecular Probes, Eugene, OR) diluted 1:500; Biotin-conjugated donkey anti-chicken (Vector Laboratories) diluted 1:200.

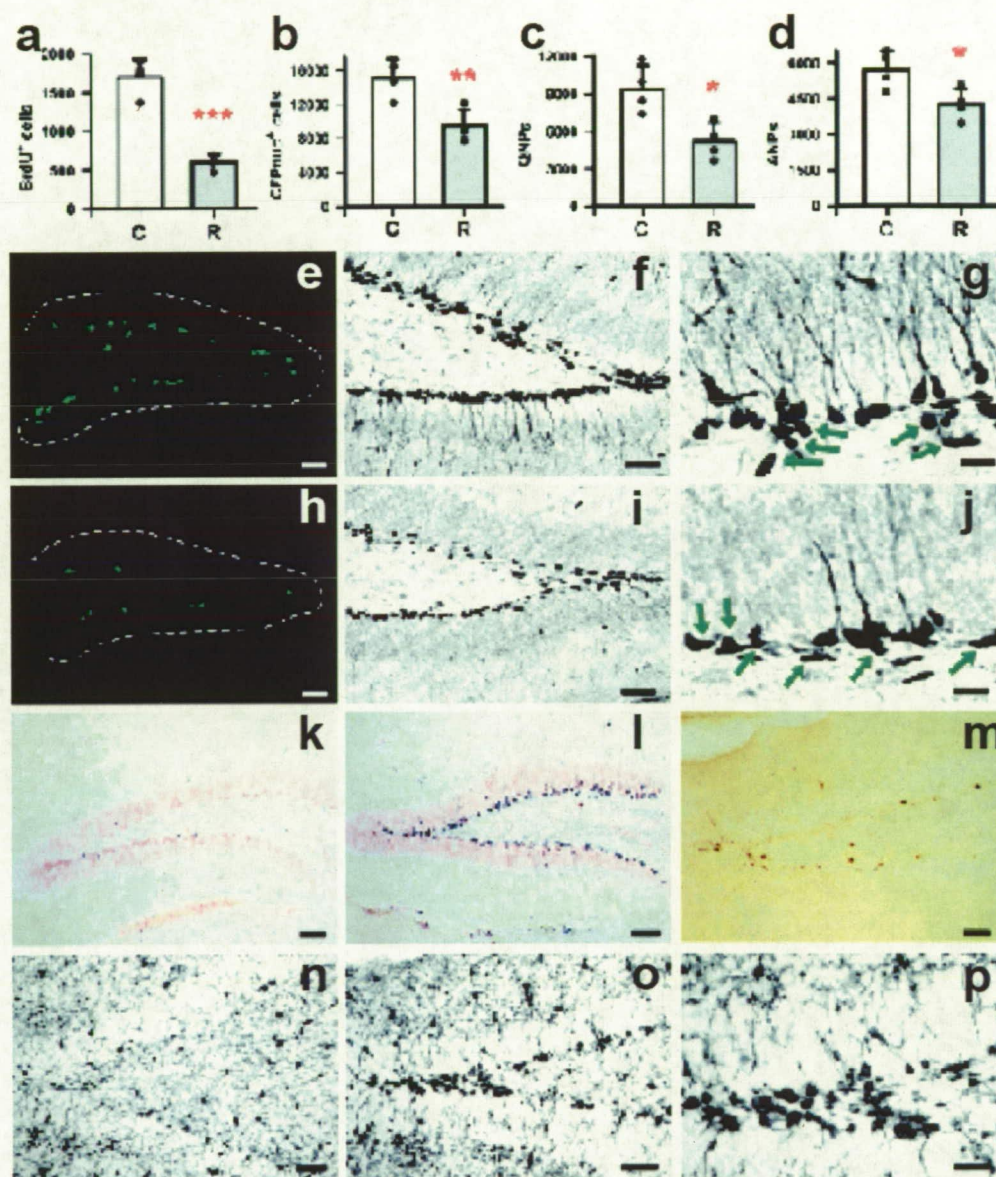
**Quantification.** Quantitative analysis of cell populations was performed by means of design-based (assumption free, unbiased) stereology (3,4). Slices were collected using systematic-random sampling. One brain hemisphere was randomly selected per animal. The hemisphere was sliced sagittally, in a lateral-to-medial direction, from the beginning of the lateral ventricle to the midline, thus including the entire DG. The 50  $\mu$ m slices were collected in 6 parallel sets, each set consisting of 12 slices, each slice 300  $\mu$ m apart from the next. All cells of each type described (BrdU<sup>+</sup>, QNPs, and ANPs) were counted in every slice under a 63x objective, excluding those in the uppermost focal plane. The number of cells from all the slices from one set were added up together, and then multiplied by 6 (the number of sets of slices per animal), thus representing the total number of cells per hemisphere; these numbers are given in the Results section. The volume of the space reference (the GCL + SGZ) was estimated using the Cavalieri-point method. All the immunostaining images were collected using an epifluorescence/bright

field microscope (Carl Zeiss, Thornwood, NY) equipped with a digital camera and the corresponding software. All images were imported into Adobe Photoshop 7.0 (Adobe Systems Incorporated, San Jose, CA) in the tiff format. Brightness, contrast, and background were adjusted using the “brightness and contrast” and “levels” controls from the “image/adjustment” set of options.

**Statistical analysis.** Statistical analysis (Student’s t-test) and graph plotting was performed using Sigmaplot 8.0 (SPSS Inc., Chicago, IL). The bars show the mean and the standard error of the mean (s.e.m), and the black dots show the data for individual animals. Differences were considered to be significant when  $p \leq 0.05$ .

## REFERENCES FOR SUPPLEMENTAL MATERIAL

1. J. M. Encinas, A. Vaahtokari, G. Enikolopov, *Proc Natl Acad Sci U S A* **103**, 8233 (May 23, 2006).
2. J. S. de Olmos, C. A. Beltramino, S. de Olmos de Lorenzo, *Neurotoxicol Teratol* **16**, 545 (Nov-Dec, 1994).
3. K. Howell, N. Hopkins, P. McLoughlin, *Exp Physiol* **87**, 747 (Nov, 2002).
4. D. A. Peterson, *Methods* **18**, 493 (Aug, 1999).



Encinas et al., Fig.1